Journal of Power Sources 185 (2008) 318–330

Contents lists available at ScienceDirect

Journal of Power Sources

journal homepage: www.elsevier.com/locate/jpowsour

DMFC performance and methanol cross-over: Experimental analysis and model validation

A. Casalegno*, R. Marchesi

Dipartimento di Energia, Politecnico di Milano, Piazza Leonardo da Vinci 32, 20133 Milano, Italy

ARTICLE INFO

Article history:
Received 3 March 2008
Received in revised form 23 June 2008
Accepted 28 June 2008
Available online 6 July 2008

Keywords:
Fuel cell
Methanol
Cross-over
Experiment
Uncertainty
Model

ABSTRACT

A combined experimental and modelling approach is proposed to analyze methanol cross-over and its effect on DMFC performance. The experimental analysis is performed in order to allow an accurate investigation of methanol cross-over influence on DMFC performance, hence measurements were characterized in terms of uncertainty and reproducibility. The findings suggest that methanol cross-over is mainly determined by diffusion transport and affects cell performance partly via methanol electro-oxidation at the cathode. The modelling analysis is carried out to further investigate methanol cross-over phenomenon. A simple model evaluates the effectiveness of two proposed interpretations regarding methanol cross-over and its effects. The model is validated using the experimental data gathered. Both the experimental analysis and the proposed and validated model allow a substantial step forward in the understanding of the main phenomena associated with methanol cross-over. The findings confirm the possibility to reduce methanol cross-over by optimizing anode feeding.

1. Introduction

Hydrogen polymer electrolyte membrane fuel cell (PEMFC) is considered a highly promising technology, especially for micropower generation and vehicular applications, due to its important attributes: low temperature and low pressure operation, no liquid electrolyte, high power density. The direct methanol fuel cell (DMFC) technology is a further development of PEMFC. Its most promising applications are portable electronics and the automotive industry, thanks to of the direct use of a high energy density liquid fuel. However, the fuel is also the cause of its main drawbacks: lower efficiency and lower power density than PEMFC. This is due to methanol permeation through the polymer membrane and the slower electrochemical methanol oxidation:

$$CH_3OH + H_2O \rightarrow CO_2 + 6H^+ + 6e^- \quad (1)$$

While oxygen reduction at cathode is similar to PEMFC:

$$\frac{3}{2}\,O_2 + 6H^+ + 6e^- \rightarrow 3H_2O \quad (2)$$

Methanol cross-over is defined as the permeation of methanol through the electrolyte membrane. State of the art membranes used in PEMFC are not fully impermeable to methanol and allow for significant quantities to permeate from the anode to the cathode. Diffusion and electro-osmotic drag are the two key mechanisms identified. When methanol reaches the cathode it is oxidized, leading to a mixed potential and an inevitable decrease in cell voltage. Moreover the oxidized methanol is effectively wasted fuel with clear negative impact in the overall efficiency of the cell. Methanol cross-over in DMFC has been recently studied both experimentally and theoretically [1]. Dohle et al. [2] and Valdez and Narayanan et al. [3] measured the methanol cross-over flux with different membrane thickness and showed that the methanol cross-over rate is inversely proportional to membrane thickness, thus indicating that diffusion is dominant. In addition, Ren et al. [4] compared diffusion with electro-osmotic drag processes and demonstrated the importance of electro-osmotic drag in methanol transport through the membrane. Valdez and Narayanan [3] and Dohle et al. [2] studied the temperature effects on methanol cross-over and showed that the methanol cross-over rate increases with cell temperature. Wang et al. [5] analyzed the chemical compositions of the cathode effluent of a DMFC with a mass spectrometer. They found that the methanol crossing over the membrane is completely oxidized to CO_2 at the cathode in the presence of Pt catalyst.

Literature references that investigate methanol cross-over mechanism and its effects show inconsistent experimental data results. The analysis are usually not characterized in terms of uncertainties and reproducibility. Thus, the evaluations and findings tend to be more qualitative than quantitative.

* Corresponding author. Tel.: +39 0223993840; fax: +39 0223993863.
E-mail addresses: andrea.casalegno@polimi.it (A. Casalegno), renzo.marchesi@polimi.it (R. Marchesi).

0378-7753/$ – see front matter © 2008 Elsevier B.V. All rights reserved.
doi:10.1016/j.jpowsour.2008.06.071

Nomenclature

c_{ref}	reference concentration (mol cm^{-3})
C	species concentration in channel (mol cm^{-3})
C_t	species concentration in catalyst layer (mol cm^{-3})
D_b	effective diffusivity in diffusion layer (cm^2 s^{-1})
D_m	effective diffusivity in membrane (cm^2 s^{-1})
E_0	ideal potential difference (V)
F	Faraday constant (C mol^{-1})
h	channel height and width (cm)
i	current density (A cm^{-2})
i_*	exchange current density (A cm^{-3})
k	Tafel constant (A cm^{-2})
l_b	diffusion layer thickness (cm)
l_m	membrane thickness (cm)
l_t	catalyst layer thickness (cm)
L	channel length (cm)
LHV	low heating value (MJ kg^{-1})
$\dot{m}$	inlet mass flow rate (g min^{-1})
n_d	water drag coefficient
n_{dx}	methanol drag coefficient
N_{cross}	cross-over flux (mol cm^{-2} s^{-1})
P	channel pressure (Pa)
R	universal gas constant (J mol^{-1} K^{-1})
R_c	contact resistance (Ω cm^2)
T	fuel cell temperature (K)
u_{cx}	cross-over measurement uncertainty (mol cm^{-2} s^{-1})
u_i	current density measurement uncertainty (A cm^{-2})
U_{tot}	total fuel utilization
V_{cell}	cell potential difference (V)

Greek

α	Tafel transport coefficient
γ	reaction order
η	polarization (V)
ηth	thermodynamic efficiency (V)

Superscript and subscript

a	relative to anode
c	relative to cathode
cross	relative to cross-over
CO_2	relative to carbon dioxide
estim	estimated
G	relative to gas phase
in	relative to channel inlet
IR	relative to internal resistance
L	relative to liquid phase
mem	relative to membrane
Met	relative to methanol
N_2	relative to nitrogen
out	relative to channel outlet
Ox	relative to oxygen

This work aims at producing a consistent and systematic set of results on methanol cross-over and its consequences on DMFC performance. The results form the basis for the increased understanding of the underlying mechanisms that regulate this phenomenon and for the development of a mathematical model.

A combined experimental and modelling approach is proposed. A systematic experimental analysis is reported; instruments are traceable to the international reference standard and measurements are characterized in terms of uncertainty and reproducibility. This complete experimental analysis allows also for a quantitative validation of the model published in [6] over a wide range of operating conditions. It is worth noticing that this aspect is generally neglected in literature. The distinctive feature of this approach is the complete model validation by three sets of experimental data: methanol cross-over, DMFC performance and anode polarization.

Both the experimental analysis and the accurate model validation allow to investigate both the transport mechanism that regulate methanol cross-over and mixed potential origin.

2. Experimental equipment and uncertainty evaluation

The experimental analyses of DMFC performance and methanol cross-over are carried out utilizing the same equipment and methodologies presented in [7]. The analyses are conducted on the same fuel cell, which has already been characterized in terms of anode polarization in a previous publication by the author [8].

The DMFC hardware, used in the following analyses, has a maximum cross-sectional area of 25 cm^{2}and a unique membrane electrode assembly (MEA) with an effective area of 12.25 ± 0.5 cm^2. The MEA is contained between two graphite blocks where fluid distributors are cut out (single serpentine channel at anode and triple serpentine at cathode, square section: depth 0.8 mm, width 0.8 mm, length 1500 mm). The cell is held together with two stainless steel plates using 8 retaining bolts, which were closed applying a torque of 12 ± 0.5 N m with a calibrated instrument.

A slot is present in the cathode steel plate to accommodate a calibrated thermocouple (uncertainty 0.05 K), connected with both a temperature controller and a data acquisition system. Two electrical heaters, connected to the temperature controller, are placed within the steel plates. There is one heater for each electrode to fully control the cell temperature. The graphite blocks present electrical contacts with gold plates, connected to a high accuracy electronic load (current uncertainty 0.25% of the effective value + 0.001 A; voltage uncertainty 0.5% + 0.001 V). The anode solution is fed by a peristaltic pump with a resolution of 1 rpm and a speed uncertainty of 0.5%; anode mass flow rate is measured with an uncertainty of 1%, thanks to a calibration that allows to relate it to pump speed. All methanol solutions are produced at the start of the experiment by mixing bi-distilled water and methanol (grade 99.5%$_{mass}$) and measuring the solution mass fractions (uncertainty 0.05%$_{mass}$) with a calibrated precision scale (uncertainty 0.1 g). The air flow rate, supplied by a compressor, is controlled and measured by a calibrated flowmeter (uncertainty 0.02 N dm^3 min^{-1}).

The MEA used in this work was purchased already assembled. The membrane is GEFC-117, anode catalysed layer presents a metal loading of 4 mg cm^{-2} (Pt:Ru = 2 wt.%), cathode catalysed layer presents a metal loading of 4 mg cm^{-2} (Pt), anode and cathode diffusion layers are carbon paper (thickness 100 μm), cell gaskets consist in a mylar layer (thickness 100 μm), in contact with the membrane, and a fibreglass layer (thickness 150 μm), covered by PTFE.

A specific data acquisition procedure was developed to determine polarization characteristics at defined operating conditions and to allow repeatable evaluations and consistent comparisons. It consist of three phases: (1) initial start-up transitory, (2) steady-state condition data acquisition and (3) final shut-down transitory. A 15 min preliminary phase, during which no data is acquired, precedes the first phase. After this preliminary phase data acquisition starts by fixing a constant voltage of 0.3 V, measuring voltage and current at 1 Hz frequency for 15 min (phase 1). The data acquisition is composed of 22 voltage measurement points, from 0.6 V to 0.1 V with a 0.05 V step. The measurements points refer to both an increasing voltage series from 0.1 V to 0.6 V and a correspond-

Table 1
Controlled. parameters of experimental sessions

Session (uncertainty)	Methanol concentration in wt.% (0.07 wt.%)	Fuel cell temperature in K (0.05 K)	Anode flow rate in g min^{-1} (1%)	Cathode flow rate in g min^{-1} (0.7% + 0.006 g min^{-1})
1	3.25	333.3	0.47	2.59
2	3.25	332.8	1.08	2.59
3	3.25	353.3	0.47	2.59
4	3.25	352.5	1.08	2.59
5	6.5	333.0	0.47	2.59
6	6.5	333.1	1.08	2.59
7	6.5	352.9	0.47	2.59
8	6.5	353.1	1.08	2.59
9	3.25	333.0	0.47	0.26
10	3.25	353.3	0.47	0.26
11	6.5	332.7	0.47	0.26
12	6.5	352.7	0.47	0.26

ing decreasing voltage series from 0.6 V to 0.1 V. The single point acquisition is performed at constant voltage, measuring voltage and current at 1 Hz frequency for 400 s. After the final transitory, similar to the initial transitory, the open circuit voltage (OCV) is acquired for 500 s at a frequency of 1 Hz. Steady-state OCV is evaluated as mean value of the last 180 s. Another procedure was developed to evaluate reproducibility: it is composed of an initial transitory and two single point acquisitions, performed at 0.4 V and 0.2 V.

Data obtained by a single point acquisition (two series of 400 values, voltage and current) are processed in 2 steps: transitory elimination and outliers elimination. The first 60 values are discarded, because resulting from the transitory caused by voltage variation. A robust method is used to individuate outliers. It eliminates values not included in the interval median ± 3 times standard deviation, estimated through median absolute deviation. Finally the last 180 points are selected as significant, then mean values of voltage and current are calculated [9,10].

Air mass flow rate influence on performance and methanol cross-over is also investigated. To minimize pressure drop and its effect on the studied quantities a triple serpentine distributor, instead of a single serpentine one, is utilized on the cathode side. Thus cathode pressure drop can be considered negligible: air pressure at fuel cell inlet and outlet is 100 ± 10 kPa. The model presented in the following sections neglects the effect of geometry variation.

Not to alter the CO_2 sensor dynamic response, the cathode outlet flow is mixed with a secondary air flow to ensure 2.59 g min^{-1}, as in previous experimental sessions.

The uncertainty associated with the measurement of electric current is evaluated according to [9,10]. The contribution of each controlled parameter is assessed considering the uncertainty of each measuring device and estimating experimentally its impact on the current measurement. The final and total uncertainty associated with the current measurement is equal to the geometric sum of the uncertainties of each controlled parameter. The single point uncertainty, u_i (179 dof, 95% population) for current density i from 0 to 0.6 A cm^{-2}, is estimated equal to:

$$u_i = -5.1 \times 10^{-2} \cdot i^2 + 2.6 \times 10^{-2} \cdot i + 3.3 \times 10^{-3} \quad (3)$$

A similar methodology is applied to evaluate methanol cross-over uncertainty. Considering operating conditions influence and CO_2 diffusion through the membrane single point uncertainty, u_{cx} (179 dof, 95% population), of methanol cross-over flux N_{cross}^{Met} from 0 to 6 ×10^{-7} mol s^{-1} cm^{-2} is estimated equal to:

$$u_{cx} = 0.03 \cdot N_{cross}^{Met} + 1.5 \times 10^{-8} \quad (4)$$

A PEMFC experimental station is utilized to define fuel cell performance and operation, in terms of cathode polarization. Hydrogen is supplied as fuel at a constant flow rate of 0.2 ± 0.002 N dm^3 min^{-1} and air is supplied at 2 ± 0.02 N dm^3 min^{-1}. The operating temperature's influence on performance is investigated, maintaining both gas saturators at equal temperature to enable an optimal membrane hydration.

The experimental methodology is very similar to that previously described and also the electric current uncertainty is evaluated considering operating conditions and the presence of hysteresis, in this case associated with water accumulation. The final uncertainty, $u_i^{H_2}$ (179 dof, 95% population) for current density i from 0 to 1 A cm^{-2}, is estimated equal to:

$$u_i^{H_2} = -1.6 \times 10^{-1} \cdot i^2 + 1.9 \times 10^{-1} \cdot i - 2.5 \times 10^{-2} \quad (5)$$

The PEMFC experimental station is adaptable to carry out hydrogen pumping [11,12], that allows the characterization of membrane proton conductivity. In this configuration, at high current density, both anode and cathode activation resistances are negligible in comparison with the fuel cell internal resistance [11]. The internal resistance is itself associated with the membrane, which gives the main contribution, and the electrodes and the contact mechanism, which can be considered negligible. Thus this methodology allows the estimation of proton membrane conductivity.

During standard PEMFC operation, with hydrogen and air feeding, anode overpotential is negligible in comparison to cathode overpotential and internal resistance. Hence once internal resistance is estimated, cathode polarization can be evaluated. It is important to note that cathode polarizations in DMFC and PEMFC operation are comparable, but a certain difference is present, due to air humidification and different water cross-over through the membrane.

3. Experimental analysis

The following experimental analysis aims at investigating the influence of operating conditions on DMFC performance and methanol cross-over, examining 12 polarization curves (Table 1).

3.1. Hysteresis

Comparing the two voltage increasing and voltage decreasing series, a hysteresis phenomenon is observed; in Fig. 1 two examples are reported. In some cases the difference between the two average current densities has a magnitude order of 10^{-2} A cm^{-2}. This is, similar to the typical single point current uncertainty. However, analysis of variance (ANOVA) confirms that in these cases the differences are significant and the two mean values have to be considered different.

Hysteresis is relevant typically at high current density and fuel utilization, in agreement with hysteresis observation in experimental anode polarization presented in [8]. It is worth noticing that the experiments presented in this work are performed utilizing

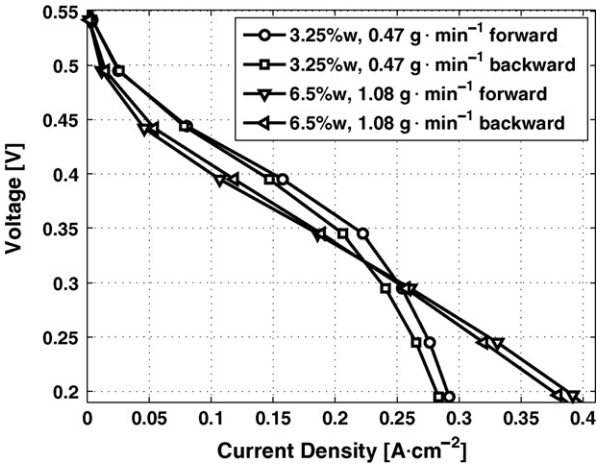

Fig. 1. Hysteresis in polarization curves. Fuel cell temperature: 333 K.

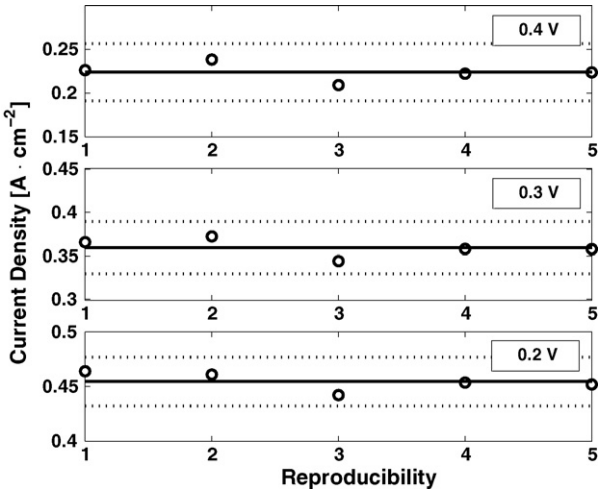

Fig. 2. Reproducibility measures in five different days. Fuel cell temperature: 353 K; methanol concentration: 6.5 wt.%; anode flow rate: 1.08 g min^{-1}.

the exact same MEA used in [8], so the set of results obtained should be directly comparable. In both cases hysteresis is present at high current density and high fuel utilization, due to methanol accumulation during operation at low current density, consistent with the explanation proposed in [8]. The complete polarization curves, presented in this work, show statistically significant hysteresis also with a high methanol concentration, up to 6.5 wt.%, differently than what observed in anode polarizations. This difference is due to a lower experimental uncertainty for complete polarization measurements, that makes smaller current differences statistically significant. Anyway hysteresis appears more intense at higher fuel utilization. In the complete polarization curves shown in Fig. 1 hysteresis presents a further morphological aspect that is not present in anode polarization. At high voltages, along the backward curve, the current density is higher than along the forward curve. Probably in these cases methanol accumulation enhances cross-over along the forward curve compared to the backward curve, where accumulation is reduced by a high utilization due to high current density. This explanation is coherent with the thesis that hysteresis is due to long-term methanol accumulation, presented in [8].

Hence hysteresis depends on the operating conditions history and has to be considered in evaluating the uncertainty of the mean values. Conservatively, the final current density uncertainty, Eq. (3), is increased by a factor of 5, compared to the single point uncertainty; in this way the hysteresis effect is no more statistically significant, as confirmed by ANOVA. Similarly methanol cross-over uncertainty is conservatively expanded to $2\% + 3.5 \times 10^{-8}$ mol s^{-1} cm^{-2}.

3.2. Reproducibility

Reproducibility is a fundamental characteristic of any experimental measurement. Consistent, reliable and valid scientific data needs to be reproducible. For each polarization curve reported in this work the measurements were carried out in five different days and data analyzed with ANOVA; in Fig. 2 is shown an example. It indicates the electric current density data obtained in different days, their average value and increased uncertainty.

Current density measurements vary over different days approximately by 10^{-2} A cm^{-2}. This is greater than the single point uncertainty. In most cases, just by evaluating single point uncertainty and without considering the increase introduced by the hysteresis factor, the ANOVA analysis reveals significant variations over different days. However, taking into account the hysteresis factor previously described, no statistically significant differences can be deduced and reproducibility is demonstrated both for current density and methanol cross-over measurements. This result confirms that the operating conditions history has to be considered in order to properly evaluate the uncertainty and reproducibility of measurements.

3.3. Comparison with previous experimental analyses

The following section presents the experimental results on fuel cell polarization and methanol cross-over flux. The experiments were conducted by varying fuel cell temperature, inlet anode flow rate and methanol concentration.

First of all it is interesting to compare the experimental results obtained with two similar fuel cells, anticipating that improved performance is expected in the fuel cell used in this work (indicated as the second). This belief originates from hydrogen conditioning, that allows to increase the availability of effective catalyst sites, as investigated in [12].

Fig. 3 shows the performances of the two fuel cells. Considering their different active areas, 19.4 cm^2 and 12.25 cm^2 and in order to assure similar fuel utilization conditions, the comparison has to be conducted at different anode flow rates, respectively, 0.7 g min^{-1}

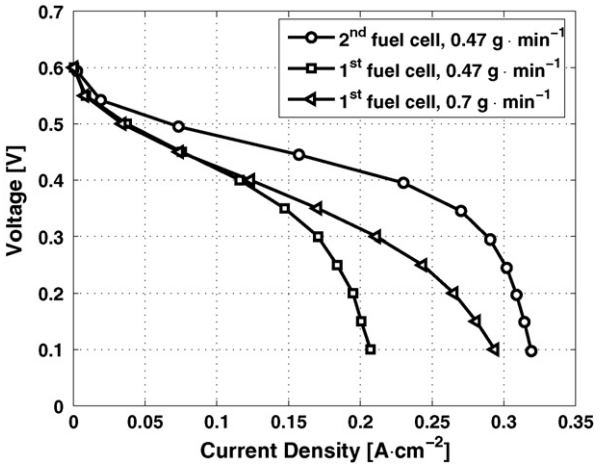

Fig. 3. Comparison of first and second fuel cells: polarization curve. Methanol concentration: 3.25 wt.%; fuel cell temperature: 353 K; different anode flow rates.

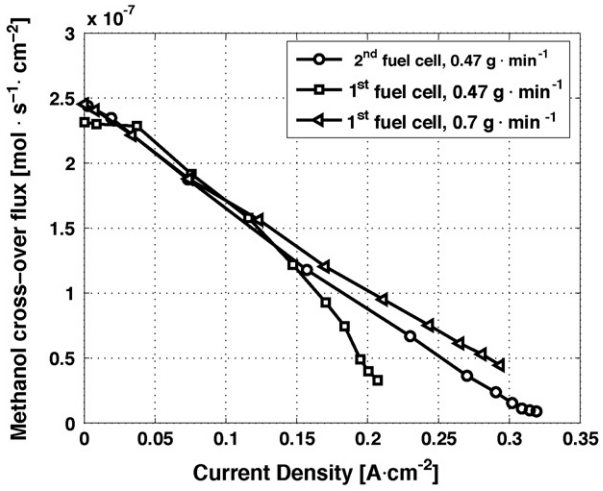

Fig. 4. Comparison of first and second fuel cells: methanol cross-over. Methanol concentration: 3.25 wt.%; fuel cell temperature: 353 K; different anode flow rates.

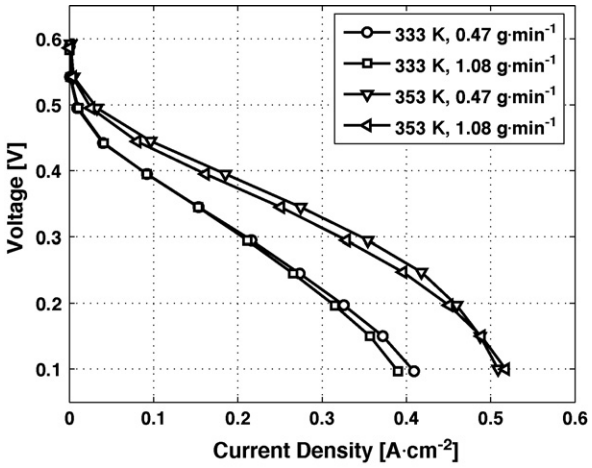

Fig. 6. Polarization curve. Methanol concentration: 6.5 wt.%; varying anode flow rate and fuel cell temperature.

and 0.47 g min^{-1}. The effectiveness of this flow rate correction is confirmed by matching limiting currents, which are associated to similar fuel utilizations. The graph clearly shows the enhanced performance of the second fuel cell, confirming the importance of the hydrogen conditioning procedure. This emphasizes again the necessity to define standard procedures in fuel cell characterization. Qualitatively, the influence of operating conditions on performance can be observed along the entire range investigated.

In Fig. 4 the comparison of methanol cross-over fluxes is also reported. The values are very similar to what would be expected and the differences are generally within the measurement uncertainty. This implies that hydrogen conditioning does not significantly affect membrane permeability of methanol. This is in line with the proposed methodology and the experimental results.

3.4. Operating conditions influence on performance and methanol cross-over

3.4.1. Influence on performance

Figs. 5 and 6 clearly show the expected positive influence of increasing temperature on fuel cell performance, mainly due to lower activation polarizations. Fig. 5 also shows that, at low methanol concentration, anode flow rate strongly influences performance, reducing limiting current density through concentration polarization; differently Fig. 6 shows that at higher methanol concentration the same variation in anode flow rate produces minor variations on performance, simply because of the excess fuel availability.

At low anode flow rate and methanol concentration, the limiting current density is mainly affected by concentration polarization, thus fuel mass transport appears as the limiting phenomenon. It is interesting to observe that in the mentioned cases the limiting current density at 353 K is significantly higher than at lower temperature, suggesting that a plausible explanation could be a higher methanol availability due to an enhancement in methanol transport in gas phase.

3.4.2. Influence on methanol cross-over

Fig. 7 shows net CO_2 fluxes, measured at cathode outlet subtracting CO_2 inlet ambient contribution; they can be related to methanol cross-over as already observed in [13,14]. At very high fuel utilization CO_2 flux is negligible, in spite of high CO_2 concentration and void fraction at anode side, that should enhance CO_2 diffusion through the membrane. Moreover, in these cases, in

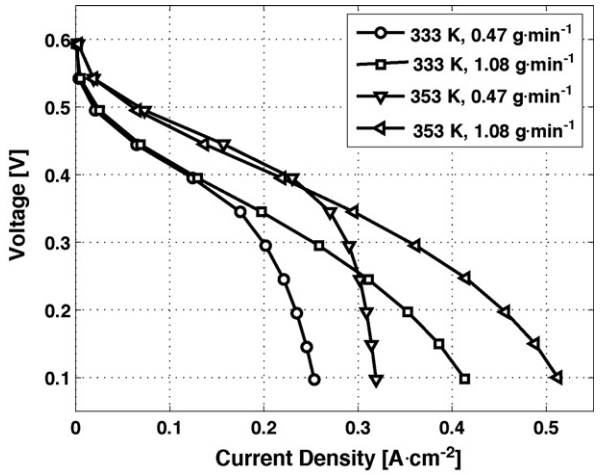

Fig. 5. Polarization curve. Methanol concentration: 3.25 wt.%; varying anode flow rate and fuel cell temperature.

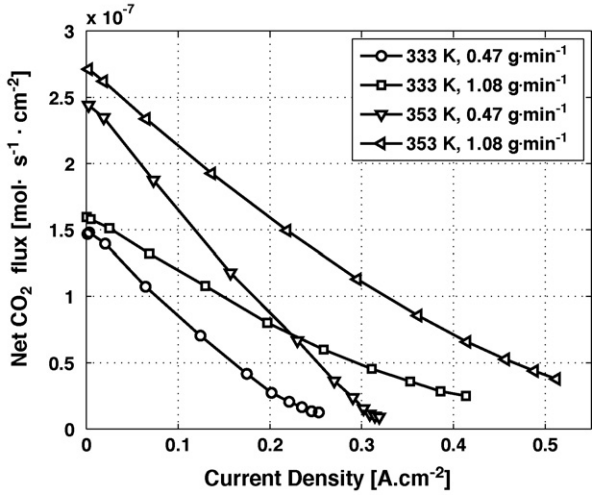

Fig. 7. Methanol cross-over flux. Methanol concentration: 3.25 wt.%; varying anode flow rate and fuel cell temperature.

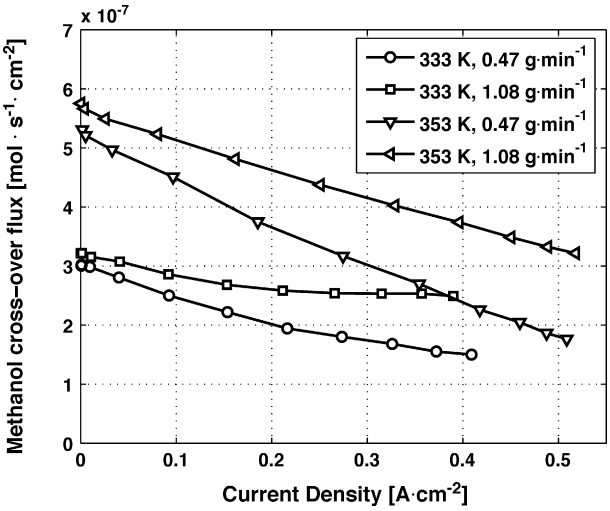

Fig. 8. Methanol cross-over flux. Methanol concentration: 6.5 wt.%; varying anode flow rate and fuel cell temperature.

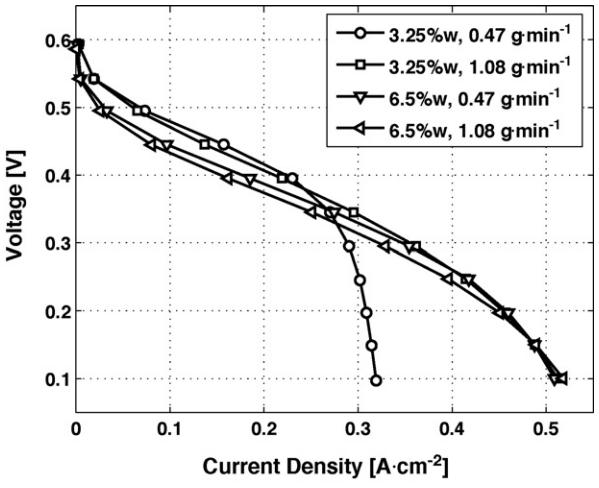

Fig. 9. Polarization curve. Fuel cell temperature: 353 K; varying methanol concentration and anode flow rate.

which methanol transport is the limiting phenomenon, methanol cross-over through the membrane is in fact negligible with respect to measurement uncertainty. These observations confirm that in the investigated operating condition, characterized by a negligible pressure difference between the electrodes, the actual CO_2 transport from anode to cathode is negligible compared to the CO_2 production due to the oxidation of cross-over methanol. This is in agreement with the interpretation reported in [13,14]. Considering that most of the methanol at the cathode is oxidized [15], the net CO_2 molar flux measured at cathode outlet is approximately equal to methanol cross-over molar flux.

Methanol cross-over flux has an approximately linear dependence on current density (Fig. 8), as already observed in [13,14]. This suggests that the contribution of electro-osmosis is minimal, since this is directly proportional to current density. Moreover, considering that the average methanol concentration in the electrode decreases more than linearly with current density, taking into account void fraction influence [8,16], methanol cross-over seems not to be dependent on the average methanol concentration in the electrode but on the methanol concentration in the liquid phase, as proposed in the developed model. A more detailed discussion of this aspect is presented in the next section.

As expected methanol cross-over is approximately proportional to inlet methanol concentration, confirming that the phenomenon is mainly due to diffusion through the membrane. This is clear when comparing high voltage data in Figs. 7 and 8. At low current densities and limited fuel utilization, anode flow rate effect on methanol cross-over is negligible, since there is no influence on local methanol concentration. At high current densities local methanol concentration is strongly determined by fuel utilization, thus anode flow rate influence becomes increasingly relevant (Figs. 7, 8 and 10). Consistently methanol cross-over is also significantly influenced by temperature, which determines the behaviour of methanol diffusion through the membrane. Quantitatively at low current density increasing fuel cell temperature from 333 K to 353 K has a similar negative effect as doubling methanol concentration.

3.4.3. *Methanol cross-over influence on performance*

In Fig. 9 polarization curves at different inlet methanol concentration and anode flow rate are reported. Excluding the curve fed by the lower inlet methanol flow rate, the others present similar limiting current densities. These are affected by cathode concentration polarization, caused by a limited oxygen transport, which is itself further reduced by water flooding of the electrode or the diffusion layer.

Analyzing the curves at low current densities, in the range of 0.1–0.2 A cm^{-2}, important differences are observable: performance is lower when increasing inlet methanol flow rate. This effect appears proportional to methanol cross-over flux (Fig. 10), suggesting it has a direct effect on the overall polarization. Considering that anode polarization has a weak dependence on methanol concentration and that no cross-over influence is observed in [8], the noticed effect appears to be related to cathode polarization.

This effect could have two origins: local concentration polarization caused by a local reduction in oxygen concentration at the cathode; or both activation and concentration polarization caused by the presence of methanol electro-oxidation at the cathode. Considering the magnitude of the phenomenon and the high air flow rate fed at the cathode, the first explanation does not seem plausible, thus only the second is taken into consideration as suggested in [16,17].

Figs. 11 and 12 show polarization and methanol cross-over curves at similar effective inlet methanol flow rate. An increase in methanol concentration produces an enhancement of cross-over

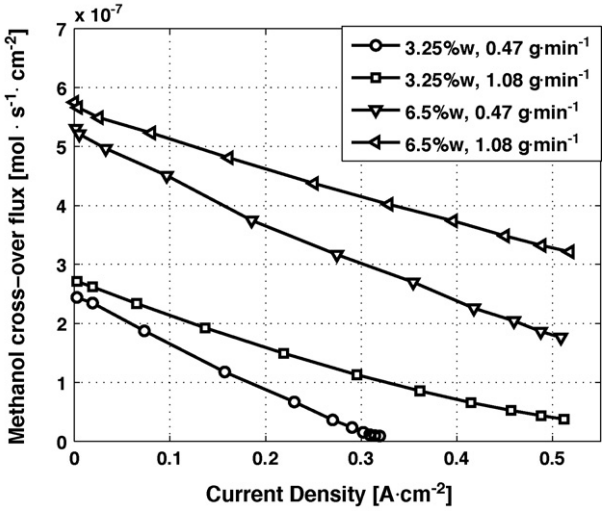

Fig. 10. Methanol cross-over flux. Fuel cell temperature: 353 K; varying methanol concentration and anode flow rate.

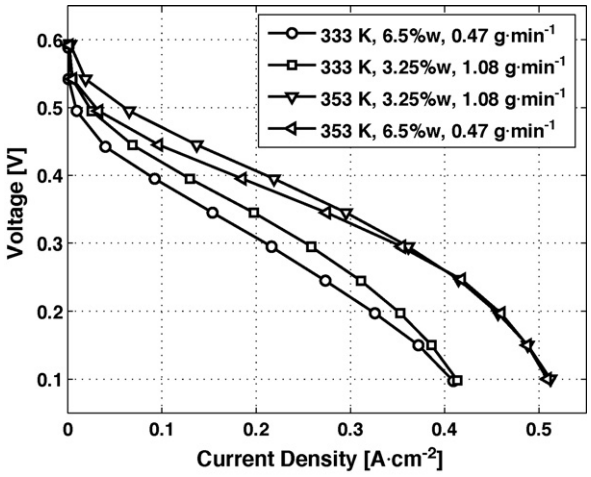

Fig. 11. Polarization curve. At similar effective methanol flow rate.

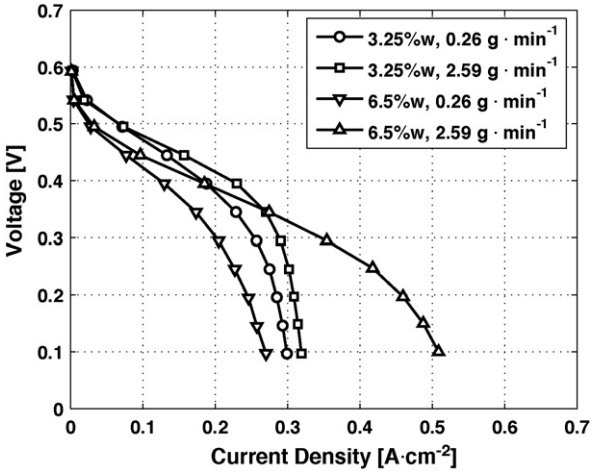

Fig. 13. Polarization curve. Fuel cell temperature: 353 K; anode flow rate: 0.47 g min^{-1}; varying methanol concentration and air flow rate.

effect, in particular at low current densities. It is interesting to observe that the magnitude of cross-over effect is considerably higher at 333 K, in agreement with a significant temperature influence on activation loss of cathode methanol electro-oxidation.

Fig. 13 shows the effect of air flow rate reduction on the polarization curve. At low methanol concentration and low anode flow rate, reducing air flow rate by a factor 10 does not considerably affect performance: the limiting current is due to methanol transport. Differently, at high methanol concentration and low air flow rate, oxygen transport is the limiting phenomenon, causing concentration polarization. Such a marked effect of air flow rate variation, not producible by the analysed increase in methanol cross-over, confirms that the first explanation previously mentioned is not satisfactory.

The effects of air flow rate reduction on methanol cross-over are shown in Fig. 14. Cross-over is lower at low air flow rate along all the operating conditions investigated. There are two plausible interpretation to explain this behaviour: cross-over due to diffusion is effectively reduced, because methanol concentration within the cathode is not anymore negligible, given a lower oxygen availability; cross-over is not reduced but is underestimated and methanol is not completely oxidized at cathode, because of lower oxygen availability, and is present at cathode outlet. Considering that Fig. 13 shows no observable effects of cross-over reduction at high voltage in Fig. 13, the second interpretation is more sound. A gas composition analysis at cathode outlet is necessary to investigate further this aspect.

3.4.4. Methanol cross-over overpotential estimation

To have a further confirmation of the cross-over effect on the polarization curve, its magnitude has been estimated through the sum of different polarizations.

The DMFC experimental polarization curve can be subdivided in anode, cathode and cross-over overpotentials, and membrane and electrode ohmic losses:

$$V_{\text{cell}} = E_0 - \eta^{\text{a}} - \eta^{\text{c}} - \eta^{\text{cross}} - \eta_{\text{mem}} - \text{Rc} \cdot i \quad (6)$$

The different overpotentials, except the methanol cross-over one, can be estimated experimentally as described below. As already stated cathode and membrane polarization estimations are not strictly equal to those present in DMFC operation, because of a different water quantity and transport. This introduces a further uncertainty in the experimental data that needs to be accounted for. Membrane and electrode ohmic losses are measured following the hydrogen pumping methodology described in [11]. The mea-

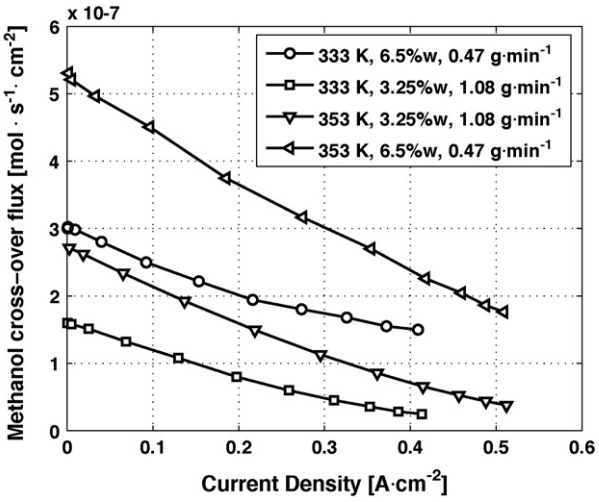

Fig. 12. Methanol cross-over flux. At similar effective methanol flow rate.

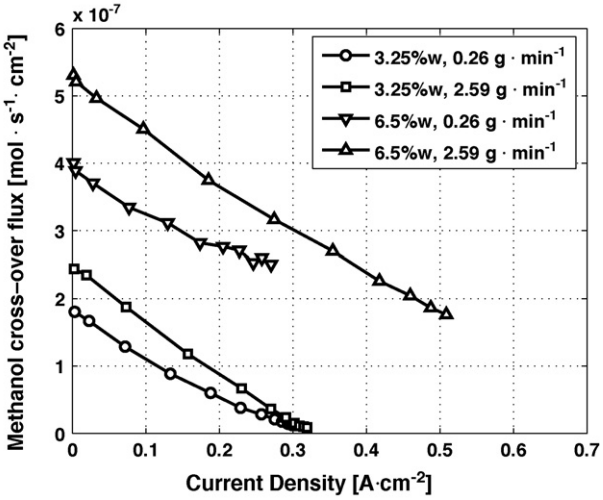

Fig. 14. Methanol cross-over flux. Fuel cell temperature: 353 K; anode flow rate: 0.47 g min^{-1}; varying methanol concentration and air flow rate.

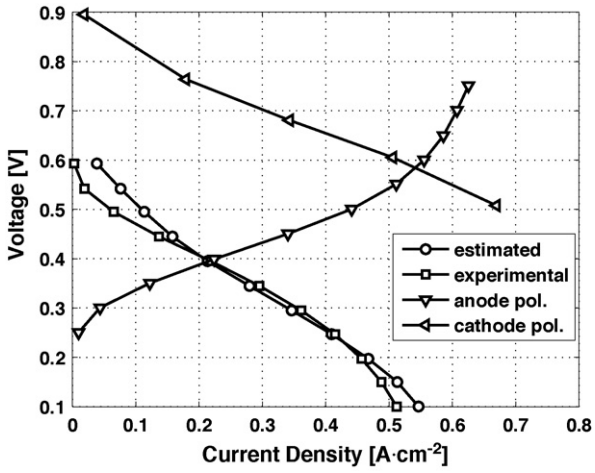

Fig. 15. Anode, cathode polarizations and experimental and estimated overall characteristic. Fuel cell temperature: 353 K; methanol concentration: 3.25 wt.%; anode flow rate: 1.08 g min^{-1}.

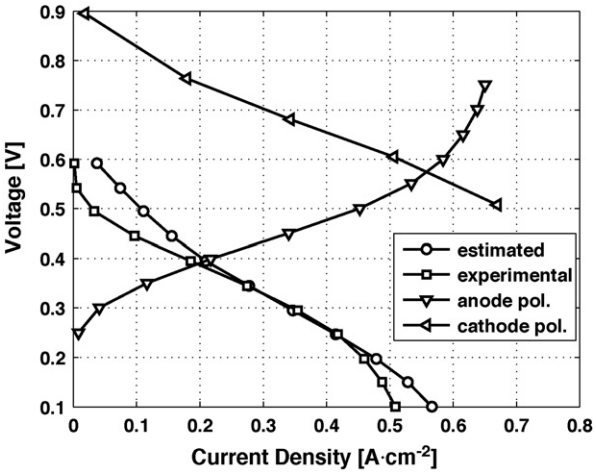

Fig. 16. Anode, cathode polarizations and experimental and estimated overall characteristic. Fuel cell temperature: 353 K; methanol concentration: 6.5 wt.%; anode flow rate: 0.47 g min^{-1}.

surements are conducted at 333 K and 353 K, feeding hydrogen saturated with water at fuel cell temperature at both anode and cathode and considering the following equation:

$$V_{\text{cell}}^{\text{IR}} = \eta_{\text{mem}} + \text{Rc} \cdot i \tag{7}$$

Proton conductivity at 333 K and 353 K is estimated equal to $0.09 \pm 0.01\ \Omega^{-1}\ \text{cm}^{-1}$ and $0.1 \pm 0.01\ \Omega^{-1}\ \text{cm}^{-1}$. This is consistent with values reported in literature [16,18,19] and does not consider perfect membrane hydration.

Cathode polarization is estimated at 333 K and 353 K, feeding hydrogen and air saturated with water at fuel cell temperature and subtracting membrane and electrode ohmic losses.

$$V_{\text{cell}}^{\text{c}} = E_0^{\text{H}_2} - \eta^{\text{c}} - \eta_{\text{mem}} - \text{Rc} \cdot i \tag{8}$$

Anode polarization is estimated starting from measurements presented in [8], conducted through methanol electrolysis and subtracting membrane and electrode ohmic losses via the following equation:

$$V_{\text{cell}}^{\text{a}} = \eta^{\text{a}} + \eta_{\text{mem}} + \text{Rc} \cdot i \tag{9}$$

Finally the overall experimental polarization curve can be compared with the estimated polarization curve that does not include methanol cross-over overpotential:

$$V_{\text{cell}} = V_{\text{estim}} - \eta^{\text{cross}} \tag{10}$$

Figs. 15 and 16 show anode polarization, cathode polarization and both experimental and estimated overall polarizations. An appreciable difference in limiting current density is evident when comparing experimental and estimated overall polarizations. This is probably caused by a higher water presence on the cathode side, due to abundant water feeding at anode in the case of DMFC configuration.

Moreover an important difference between estimated and experimental DMFC polarizations at low current densities confirms the presence and the order of magnitude of a direct and consistent methanol cross-over effect. In fact estimating the overall characteristic by sum of the polarizations allows excluding cross-over effect. This conclusion can be drawn by noticing that methanol permeation through the membrane is present only in methanol electrolysis measurements, where both cathode related polarization and cathode cross-over effect are negligible.

Comparing Fig. 15 with Fig. 16, which has increased inlet methanol concentration but similar inlet methanol flow rate, cross-over effect appears higher. This is in agreement with previous comments related to Figs. 9 and 10.

3.4.5. Open circuit voltage analysis

Fig. 17 shows the open circuit voltages (OCV) corresponding to all the different experiment sessions listed in Table 1. Open circuit voltage is strongly influenced by cathode mixed potential. The data clearly shows that high methanol concentration produces an important reduction of OCV, determining an increase in methanol cross-over.

A temperature increase produces two effects: an increment of methanol cross-over; an enhancement in methanol oxidation kinetics at cathode. These effects have opposite influences on cathode mixed potential. In fact an increase of temperature produces limited positive effects on OCV only at low methanol concentration, in spite of an increase in methanol cross-over. Methanol oxidation at cathode can occur via a chemical or electro-chemical mechanism. The chemical kinetics, associated with the two mechanisms, are enhanced differently by a temperature increase, probably compensating the increment in methanol cross-over. As expected instead, the influence of anode flow rate on OCV is negligible.

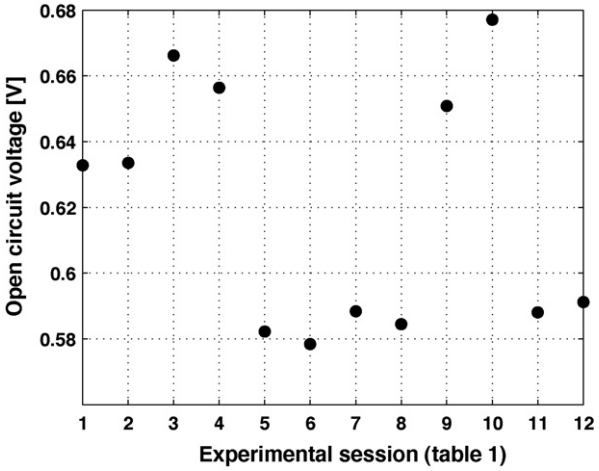

Fig. 17. Open circuit voltage of experimental sessions (Table 1); estimated uncertainty: 0.01 V.

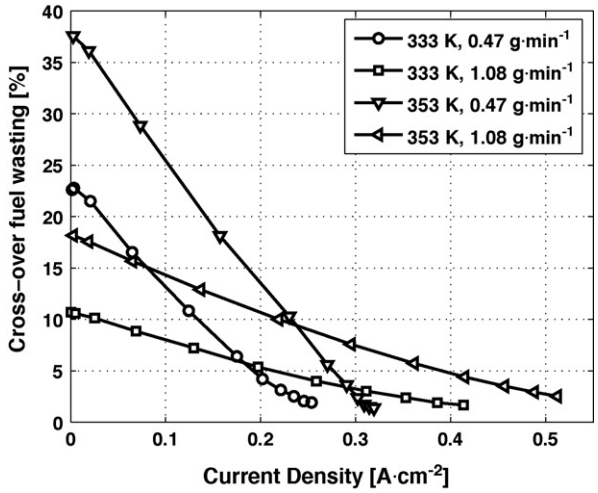

Fig. 18. Cross-over fuel wasting. Methanol concentration: 3.25 wt.%; varying anode flow rate and fuel cell temperature.

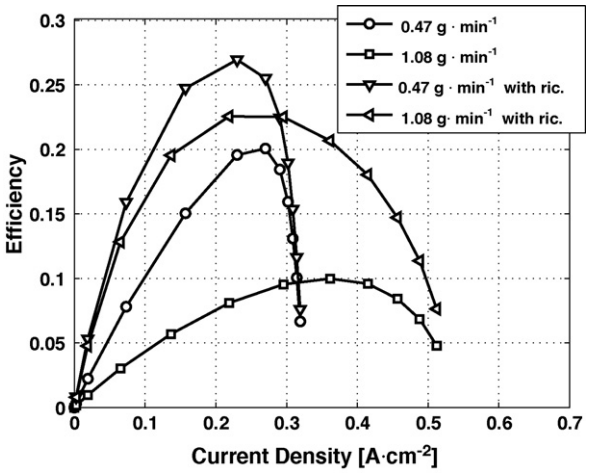

Fig. 19. Efficiency with and without fuel recirculation. Fuel cell temperature: 353 K; methanol concentration: 3.25 wt.%; varying anode flow rate.

At lower air flow rates OCVs are very similar, with only a slight increase observable at lower temperature. These results seem to confirm the previously proposed interpretation: the significant reduction of methanol cross-over is apparent, the low oxygen availability determines methanol presence in cathode stream.

OCV analysis confirms the existence of a direct methanol cross-over influence on DMFC performance, probably caused also by methanol electro-oxidation at cathode side.

3.4.6. Methanol cross-over influence on efficiency

Another important consequence of methanol cross-over is fuel wasting. Also at low inlet methanol concentration it can be over 20% of fed fuel (Fig. 18). The clear consequence is a significantly reduced fuel cell efficiency. To evaluate fuel cell performance two efficiencies are analysed:

- thermodynamic efficiency as the ratio between produced electrical power and inlet chemical power:

$$\eta\mathrm{th} = \frac{V_{\mathrm{cell}} \cdot I}{\dot{m}_{\mathrm{met}} \cdot \mathrm{LHV}_{\mathrm{met}}} \tag{11}$$

  where $\dot{m}_{\mathrm{met}}$ is the inlet methanol flow rate
- efficiency with fuel recirculation as the ratio between produced electrical power and utilized chemical power:

$$\eta_{\mathrm{ric}}^{\mathrm{th}} = \frac{V_{\mathrm{cell}} \cdot I}{\dot{m}_{\mathrm{met}} \cdot U_{\mathrm{tot}} \cdot \mathrm{LHV}_{\mathrm{met}}} \tag{12}$$

  where U_{tot} is the total fuel utilization, including the fractions used in the electrochemical reaction and wasted with methanol cross-over.

In Figs. 19 and 20 both efficiencies are reported as a function of current density, for measurements effectuated at inlet methanol concentration of 3.25%, characterized by higher efficiencies than with increased methanol concentration.

The maximum values of efficiency with and without fuel recirculation are obtained at 353 K and 0.47 g min^{-1}, respectively, 27% (90 mW cm^{-2}) and 20% (95 mW cm^{-2}). Thus fuel recirculation appears effective to improve fuel cell efficiency. In spite of lower absolute efficiency values its effect is enhanced at lower fuel cell temperature, due to a lower cross-over, and at higher anode flow rate, due to a lower total fuel utilization.

Fuel wasting is still considerable, included between 5% and 10% of inlet methanol flow rate, also in the conditions that maximize the efficiencies, confirming the important negative effect of methanol cross-over.

4. Model validation

4.1. Model description

The following analysis regards a model already presented and discussed in [6,8]. There it is already stated that the model does not pretend to be a rigorous and exhaustive description of complex DMFC behaviour, but aims to reproduce the main involved phenomena and hence to be a tool for DMFC understanding and optimization. Some more complex models are more accurate in describing fuel cell behaviour in certain specific conditions [6], instead this model is able to simulate DMFC in a wide range of operating conditions, permitting a complete quantitative validation, generally neglected in the literature. In this work the model is further validated and used to investigate methanol cross-over and its effect on performance.

Two variants are here adopted in Eqs. (13) and (15), in respect of the original model [6], as a first intent to include cross-over methanol electro-oxidation at cathode side and to better describe methanol electro-osmosis.

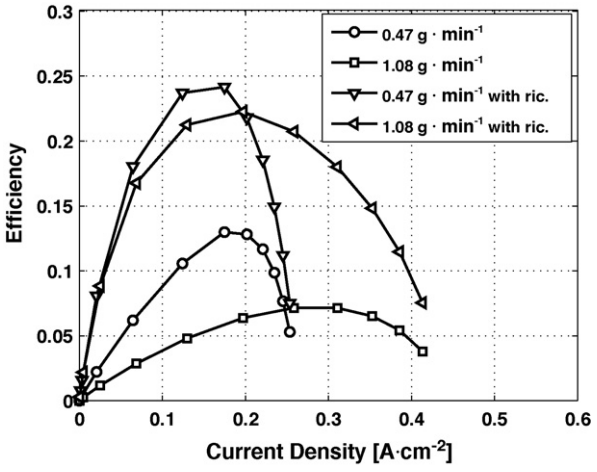

Fig. 20. Efficiency with and without fuel recirculation. Fuel cell temperature: 333 K; methanol concentration: 3.25 wt.%; varying anode flow rate.

Table 2
Geometrical parameters

h^a	0.08	[cm]
h^c	0.08	[cm]
L	76.6	[cm]
l_b^a	0.01	[cm]
l_b^c	0.01	[cm]
l_t^a	0.001	[cm]
l_t^c	0.001	[cm]
l_m	0.018	[cm]

Cathode polarization is assumed to have Tafel kinetic of order γ^c, depending on oxygen concentration in the catalyst layer:

$$\eta^c = \frac{RT}{\alpha^c F} \cdot \ln\left(\frac{i + 6 \cdot F \cdot N_{cross}^{Met}}{k^c}\right) \quad (13)$$

$$k^c = i_*^c \left(\frac{C_{t,O_2}}{c_{ref}^c}\right)^{\gamma^c} \quad (14)$$

Eq. (13) has been modified, adding the term $6 \cdot F \cdot N_{cross}^{Met}$ to current density, with the intent to provide a possible description of methanol electro-oxidation at cathode side, as proposed in [16]. The proposed equation assumes that methanol is completely depleted in cathode electrode by a electro-chemical reaction with oxygen, characterized by a rate determining step equal to oxygen electro-reduction.

Methanol and water cross-over are due to liquid phase diffusion and electro-osmosis. Water and methanol concentrations at cathode side are negligible, in comparison to anode concentrations. Water concentration in the catalyst layer is assumed equal to anode channel one and, for the purpose of electrosmotic flux calculation, water molar fraction in the catalyst layer is assumed equal to 1.

$$N_{cross}^{Met} = \frac{D_m^{Met}}{l_m} \cdot C_t^L + n_{dx} \cdot \frac{i}{F} \cdot \frac{C_t^L}{C_{H_2O}^{a,L}} \quad (15)$$

Eq. (15) differs by the presence of a specific methanol drag coefficient, n_{dx}, different from water drag coefficient, n_d. These parameters will be discuss in the following section.

The system presents 7 differential equations, 22 algebraic equations, 29 variables. This DAE system can be solved numerically applying the appropriate initial conditions, regarding inlet flows, fuel cell temperature and potential difference. Total and mean electrical current and cross-over flows can be calculated by integration over MEA area. Thus the relations, commonly used to characterize direct methanol fuel cells, are obtained: polarization and methanol cross-over curves. For this work Matlab® environment was used to solve the DAE system.

Table 3
Experimental conditions

P^a	101325	[Pa]
P^c	101325	[Pa]
T	333, 353	[K]
$\dot{m}^a$	0.47, 1.08	[g min^{-1}]
$\dot{m}^c$	2.59	[g min^{-1}]
C_{met}^0	3.25, 6.5	[wt.%]
V_{cell}	0.3–0.6	[V]

Table 4
Assumed parameters

α^c	K_1	
D_b^c	K_4	[cm^2 s^{-1}]
D_m	$K_5\, e^{K_6(\frac{1}{303} - \frac{1}{T})}$	[cm^2 s^{-1}]
i_*^c	$K_2\, e^{\frac{K_3}{R}(\frac{1}{353} - \frac{1}{T})}$	[A cm^{-2}]
n_{dx}	$K_7\, e^{1029(\frac{1}{333} - \frac{1}{T})}$	

Table 5
Fitting parameters

K_1	0.6	
K_2	1.37×10^{-4}	[A cm^{-2}]
K_3	50750	[J mol^{-1}]
K_4	7.5×10^{-3}	[cm^2 s^{-1}]
K_5	1×10^{-6}	[cm^2 s^{-1}]
K_6	3488	[K]
K_7	0.87	

4.2. Validation

The quantities present in the model have physico-chemical meaning, there are no pure adaptive parameters. These quantities are divided in: geometrical parameters, defined by the experimental hardware, shown in Table 2; operating conditions, defined by experimental analysis, presented in Table 3; some assumed parameters are reported in Table 4, the remaining are determined through validation with anode polarization measurements or assumed from literature [8]; fitting parameters (Table 5).

The calibration procedure consists in minimization of the residuals between model estimation and experimental results in the complete investigated range of operating conditions. The utilized experimental data are composed of 56 current density measures and 56 methanol cross-over flux measures, coming from 8 polarization curves, previously presented (sessions 1–8 of Table 1), at different temperature, inlet methanol concentration and inlet anode flow rate. Considering that the potential difference range interesting for applications is from 0.6 V to 0.3 V, the model and the calibration procedure were developed to produce a more accurate fitting in this range. Experimental results at lower voltages and lower air flow rate are not considered, because this simple model is not able to simulate properly such conditions, where water flooding at cathode may occurs and complex two-phase fluid dynamics aspects may be important, as already stated in [6]. The first four fitting parameters (Table 5), characterize cathode kinetics and effective oxygen diffusivity through diffusion layer and are obtained by minimization of the residuals between model estimation and current density measures.

The fitting parameters, K_1, K_2 and K_3, characterize cathode kinetics, composed of quantities affected by uncertainty, demonstrated by a consistent variability in literature [16,18,20,21]. Compared to the latter the values resulting from calibration are reasonable, in particular K_1, cathode transfer coefficient is generally included in

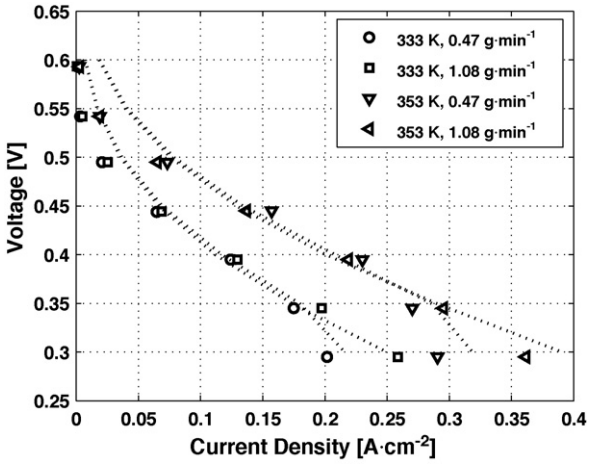

Fig. 21. Polarization curve experimental (points) and modelling (lines). Methanol concentration: 3.25 wt.%; varying fuel cell temperature and anode flow rate.

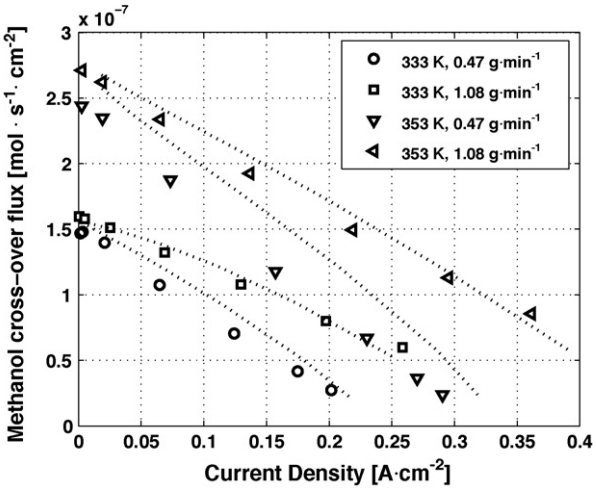

Fig. 22. Methanol cross-over flux experimental (points) and modelling (lines). Methanol concentration: 3.25 wt.%; varying fuel cell temperature and anode flow rate.

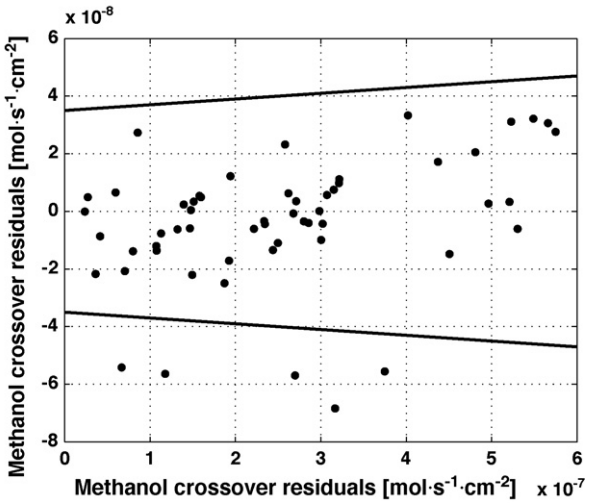

Fig. 24. Methanol cross-over residuals. Experimental uncertainty in solid line.

the range 0.5–0.9, and K_3, activation energy, is around 70 kJ mol^{-1}. Considering the contribution of gas diffusion layer porosity, tortuosity and possible water flooding effective oxygen diffusivity through diffusion layer, K_4, is an uncertain parameter. The fitting value is coherent with the values present in literature, where it is generally included in the range 10^{-3} to 10^{-2}cm^2 s^{-1}.

The last three fitting parameters (Table 5), characterize methanol cross-over through the membrane and are obtained by minimization of the residuals between model estimation and methanol cross-over flux measures. The fitting parameters K_5 and K_6 describe methanol diffusivity through the membrane. The fitting value are reasonable and very similar to those reported in [22]. K_7 is methanol drag coefficient, the fitting value, 0.87, lower than water drag coefficient at the same temperature, 2.9, suggests that methanol affinity to proton is lower than water or that methanol concentration gradient in the electrode influences electro-osmosis.

The residuals produced in the investigated interval, 0.3–0.6 V, between model estimation and experimental current density have reasonably normal distribution and absolute values lower than 0.03 A cm^{-2}, an example is reported in Fig. 21. Analogously residuals between model estimation and experimental methanol cross-over flux have reasonably normal distribution and absolute values lower than 6×10^{-8}A cm^{-2}, examples are reported in Fig. 22.

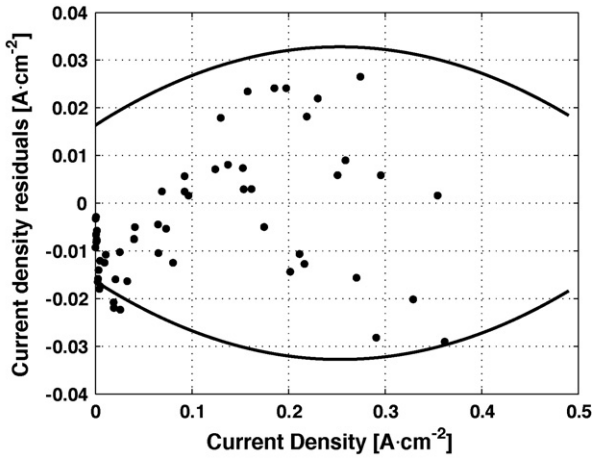

Fig. 23. Current density residuals. Experimental uncertainty in solid line.

An accurate residual analysis has been effectuated, evaluating them in comparison with experimental uncertainty. In Figs. 23 and 24 the residuals are reported in function of current density, with relative experimental uncertainty. Model accuracy is evaluated quantitatively by *F*-test, as reported in [23]. It verifies if the model is sufficiently accurate, in comparison to experimental uncertainty, to consider the latter as confident interval of model estimation.

Experimental measures of both current density and methanol cross-over from 0.3 V to 0.6 V satisfy *F*-test (95%), thus in this range the model results accurate in reproducing fuel cell behaviour and validated for prediction, maintaining experimental uncertainty as prediction confidence interval. This implies that the phenomena neglected with the proposed assumptions have minor effects, considering experimental uncertainty. Measures with a lower uncertainty are necessary for a further evaluation of model accuracy. Instead below 0.3 V the model results less accurate, implying that predictions in that range have an error higher than experimental uncertainty as commented in [6].

Fitting has been carried out also without the two variants proposed in Eqs. (13) and (15). The obtained fitting values do not differ substantially, but the model results much less accurate in

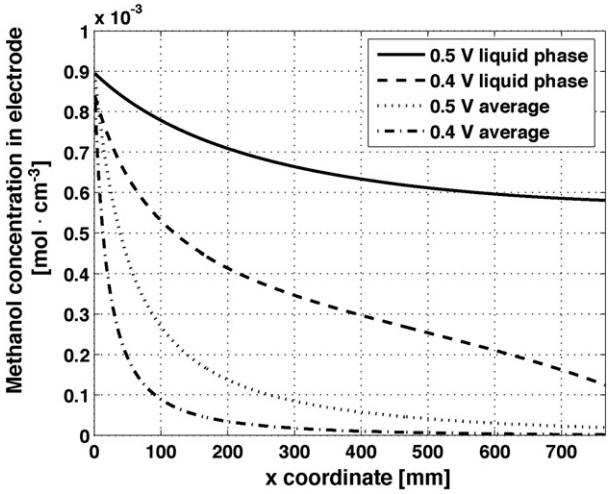

Fig. 25. Methanol concentration in electrode. Methanol concentration: 3.25 wt.%; anode flow rate: 0.47 g min^{-1}; fuel cell temperature: 353 K.

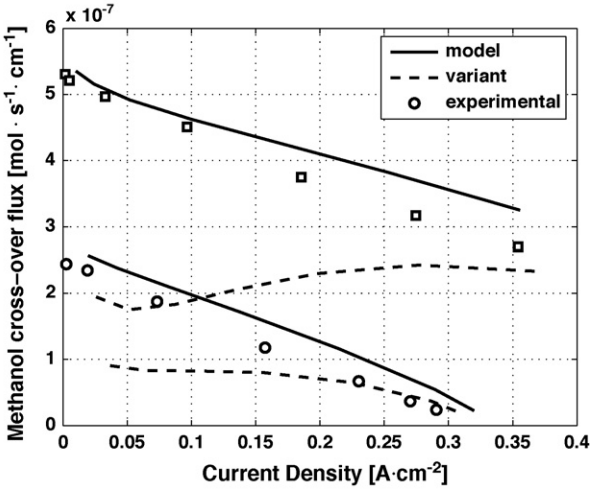

Fig. 26. Methanol cross-over fluxes, experimental data, model estimations. Methanol concentration: 3.25 wt.% (square), 6.5 wt.% (round); anode flow rate: 0.47 g min^{-1}; fuel cell temperature: 353 K.

describing fuel cell behaviour, in particular at low current densities, and residual analysis do not satisfy *F*-test. This is a further confirmation that the presented interpretation and adopted model variants are reasonable.

Considering the difficulties to produce local measures in fuel cell research, in future work we intend to produce different and more accurate global quantities measurements, in particular evaluating the influence of components properties and geometries, in order to obtain model improvements and further validations.

4.3. Estimated quantities discussion

Void fraction strongly affects average methanol concentration in the anode electrode (Fig. 25), in fact concentration in liquid phase is considerably higher than the average value. Moreover concentration in liquid phase decreases along the channel much less steeply than average concentration. This has a very important impact in determining methanol cross-over. In the described model the diffusion term of cross-over depends on methanol concentration in liquid phase, Eq. (15), but could depend on average concentration. To confirm the validity of that assumption in Fig. 26 experimental data are compared with the model and this possible variant. The proposed assumption produces a much more accurate description

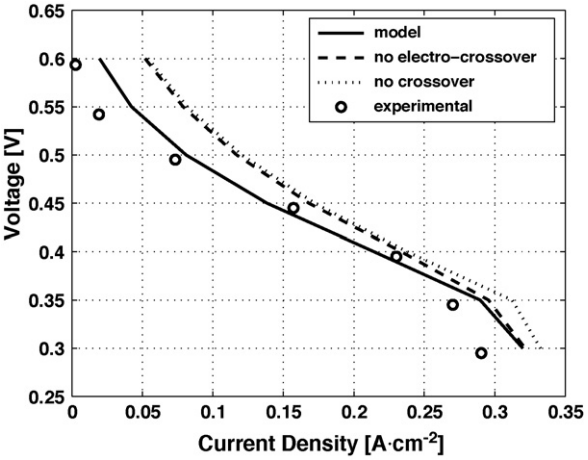

Fig. 27. Effect of methanol cross-over on polarization curve. Methanol concentration: 3.25 wt.%; anode flow rate: 0.47 g min^{-1}; fuel cell temperature: 353 K.

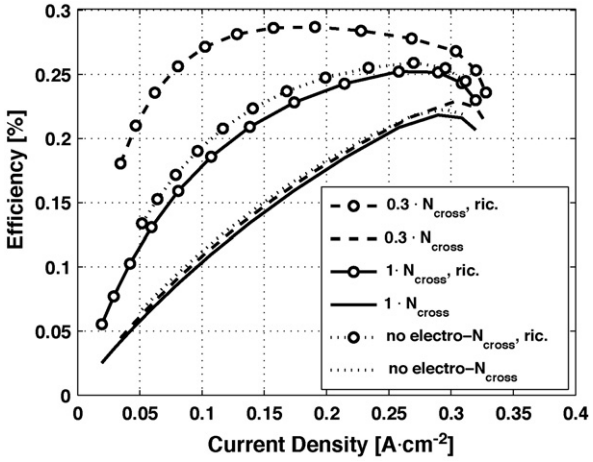

Fig. 28. Effect of methanol cross-over on fuel cell efficiency, with or without recirculation. Methanol concentration: 3.25 wt.%; anode flow rate: 0.47 g min^{-1}; fuel cell temperature: 353 K.

of methanol cross-over behaviour, confirming that the latter mainly depends on concentration in liquid phase and may be reduced optimizing methanol transport through diffusion and catalyst layers, as also suggested in [8].

The validated model permits to analyze the effect of methanol cross-over on polarization curve. The proposed hypothesis of methanol electro-oxidation allows a better fitting of experimental results compared to a model variant that excludes it (Fig. 27). Moreover it is interesting to note that the differences between these two cases are very similar to those regarding experimental measures, presented in Figs. 15 and 16. This is a further confirmation of the proposed interpretation, that permits to describe the strong effect observed experimentally at low current densities, as a consequence of methanol cross-over.

Finally an efficiency analysis is carried out through the model, evaluating two hypothetical cases (Fig. 28): in the first cross-over is reduced to 30% of original value; in the latter no methanol electro-oxidation at cathode side occurs. If fuel recirculation is not adopted very limited effects are appreciable in both cases. A reduction of cross-over to one third, in the case with fuel recirculation, produces a much more evident increase in DMFC efficiency than excluding methanol electro-oxidation at cathode. This implies that, especially at high current density, the major contribution in reducing fuel cell efficiency is due to fuel wasting and is not imputable to the eventual presence of methanol electro-oxidation at cathode. At low current density the presented interpretation evidences that the reduction of this parasitic reaction has positive effect in order to increase DMFC efficiency.

5. Conclusions

The analysis presented in this work produces the following conclusions:

- A systematic experimental analysis of operating conditions influence on performance and methanol cross-over is presented, characterizing measurements in term of uncertainty and reproducibility.
- The experimental analysis permits to verify previous experiences and interpretations, also regarding hysteresis presence, to confirm the positive effect of hydrogen conditioning on performance, to investigate accurately the direct influence of methanol cross-over on performance.

- Combining the experimental results obtained with different station configurations, methanol cross-over overpotential is estimated and investigated. It is probably caused by a methanol electro-oxidation at cathode.
- A developed DMFC model has been modified and calibrated in an extensive operating condition range, utilizing 56 current density measures and 56 methanol cross-over measures, coming from 8 polarization curves, and determining 7 fitting parameters.
- The model is able to reproduce accurately both DMFC performance and methanol cross-over flux in the investigated range. The obtained values of fitting parameters and local quantities estimation are coherent with the literature and the residuals between model estimations and experimental results are lower than measurement uncertainty.
- The effectiveness of two proposed interpretations regarding methanol cross-over and its effect is evaluated. The model, including the proposed interpretations, permits to describe more accurately experimental results.
- The systematic experimental analysis and the accurate and extensive model validation contribute to the understanding of the main phenomena involved and to confirm the necessity of methanol cross-over reduction, in order to enhance considerably DMFC performance, and the possibility of such reduction optimizing anode feeding.

Acknowledgements

The authors would like to thank Luca De Lorenzo and Fabio Di Fonzo for the useful discussions.

References

[1] A. Heinzel, V.M. Barragan, J. Power Sources 84 (1999) 70–74.
[2] H. Dohle, J. Divisek, J. Mergel, H.F. Oetjen, C. Zingler, D. Stolten, J. Power Sources 105 (2) (2002) 274–282.
[3] T.I. Valdez, S.R. Narayanan, Proceedings of the 194th Meeting of the Electrochemical Society, Boston, November 1998.
[4] X. Ren, T.E. Springer, T.A. Zawodzinski, S. Gottesfeld, J. Electrochem. Soc. 147 (2000) 466.
[5] J.T. Wang, S. Wasmus, R.F. Savinell, J. Electrochem. Soc. 143 (1996) 1233.
[6] A. Casalegno, R. Marchesi, D. Parenti, Fuel Cells (2008) 37.
[7] A. Casalegno, R. Marchesi, F. Rinaldi, ASME J. Fuel Cell Sci. Technol. 4 (2007) 418.
[8] A. Casalegno, R. Marchesi, J. Power Sources 175 (2008) 372.
[9] Env 130051999, BIPM, IEC, IFCC, ISO, IUPAC, IUPAP, OIML, International Organization for Standardization, 1993, ISBN 92-67-10188-9.
[10] B.N. Taylor, C.E. Kuyatt, NIST Technical Note 1297, National Institute of Standards and Technology, 1994.
[11] F. Barbir, H. Gorgun, J. Appl. Electrochem. 37 (2007) 359.
[12] Z. Xu, Z. Qi, C. He, A. Kaufman, J. Power Sources 156 (2006) 315.
[13] A. Casalegno, P. Grassini, R. Marchesi, Appl. Therm. Eng. 27 (2007) 748.
[14] V. Gogel, T. Frey, Z. Yongsheng, K.A. Friedrich, L. Jšrissen, J. Garche, J. Power Sources (2004) 172.
[15] H. Dohle, J. Divisek, J. Mergel, H.F. Oetjen, C. Zingler, D. Stolten, J. Power Sources 105 (2002) 274.
[16] Z.H. Wang, C.Y. Wang, J. Electrochem. Soc. 150 (2003) 508.
[17] C.H. Chen, T.K. Yeh, J. Power Sources 160 (2006) 1131.
[18] K. Scott, W. Taama, J. Cruickshank, J. Power Sources 65 (1997) 159.
[19] F. Damay, L.C. Klein, Solid State Ionics 162-163 (2003) 261.
[20] A.A. Kulikovsky, Electrochem. Commun. 7 (2005) 237.
[21] H. Guo, C.F. Ma, Electrochem. Commun. 6 (2004) 306–312.
[22] H. Dohle, J. Divisek, R. Jung, J. Power Sources 86 (2000) 469–477.
[23] D.M. Himmelblau, Process Analysis by Statistical Methods, Wiley & Sons, 1970.